# Autocatalytic colloid suspensions in the presence of a liquid-liquid interface

Author: Lucas Santiago Palacios Ruiz.
*Facultat de Física, Universitat de Barcelona, Diagonal 645, 08028 Barcelona, Spain*.*

Advisor: Ignacio Pagonabarraga Mora and Samuel Sánchez Ordoñez.

**Abstract**: Self-propelled diffusiophoretic colloids are currently being studied because of its revolutionary way to solve real applications on fields such as water cleaning or medicine. One of the most considered prototypes is the Pt-silica Janus because of its simplicity and easy construction. Although today Janus can be built within hours, still it lacks some physical knowledge of their behaviour. In an attempt to understand better Janus, in this project I have performed not only an experimental but also a computational approach to Janus. In particular, I have focus on what happens for Pt-silica Janus in a dilute regime near a liquid-liquid interface. Experimental results have shown how the velocity is decreased compared to its usual velocity on bulk up to 45%. Moreover, interface modifications with surfactants has also shown how on the one hand, surfactants interfere in Janus velocity but also, how Janus are further to the interface. Computational results, could not approximate as much as experimental, but at least they show how Janus can be modelled and how this model could explain real behaviour of Janus at the bulk by selecting a small region for chemorepellant mobility parameters related to each of the parts of the Janus particle.

## I. INTRODUCTION

In the last days of 1959, Richard Feynman introduced the idea of tiny machines as nanofactories that could perform autonomous actions in coordination with millions of other similar machines [1]. Since then, the ideas of tiny machines have become commonplace in science fiction as one could see in films such as "Fantastic Voyages", "Honey, I shrunk the kids" or even more recently, in "Big Hero 6". Nowadays, where miniaturization of technology has been a hot topic, the idea of Feynman is not far from being real. New physical approaches from active matter studies could potentially make this idea as real as laser technology is today.

Active matter is any system where exist a large number of autonomous agents that could transform energy into work [2]. Therefore, as they continuously consume energy, these systems must be out of thermal equilibrium. Typically, these systems are composed by self-propelled agents that move inside a fluid. In order to make this possible, agents transform the consumed energy into kinetic energy, allowing them to move by them-selves inside the fluid. It is important to notice that in these systems, the direction of self-propelled motion is not fixed by an external field but because of anisotropy of the agent [2]. Although the idea of having a system with billions of these self-propelled agents could be difficult to imagine, in fact, active matter is very present in nature, especially in biology. For instance, one could think of a bacterium, a cell or a major animal as one of these self-propelled agents [2]. Recently, improvements in nanotechnology have led to the creation of artificial self-propelled units. In the last years, a number of different approaches have been used to fabricate these self-propelled particles. One of the most used artificial agents is the "Janus" particle. Janus particles are micro or nanospheres with the property of having their surface split in two different materials, leading to different physical properties on each of the parts (see Fig. 1). In past years, this type of particles has been done to obtain a particle with a hydrophilic and a hydrophobic part [3]. More recently, a new use has been established for these particles. Instead of making it amphiphilic, it has been used for catalysing different reactions in each of the two parts of the Janus particle. As a consequence of the heterogeneous catalysis, a flow is established around the particle. Different strategies have used to describe these flows [4]. Nevertheless, the main idea is to obtain anisotropy in the spherical particle leading to self-propulsion. The simplest way of achieving it is by making possible a catalytic reaction in only one of the two parts. In this type of Janus particles, the part that catalyses the reaction is known as the active part and the other half, the passive one. Usually, active part of the Janus particle is made of Pt and the inactive part of silica ($SiO_2$). In the presence of $H_2O_2$, Pt catalyses the following reaction:

$$H_2O_2 \xrightarrow{Pt} H_2O + {}^1\!/_2\, O_2$$

Reaction 1. Decomposition of $H_2O_2$ in the presence of Pt.

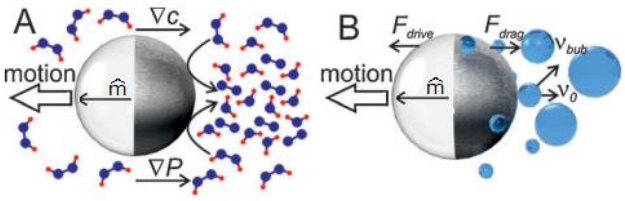


FIG. 1: Pt (grey part)-Silica (white part) Janus particle. Movement can be described by self-diffusiophoresis (A) or by bubble propulsion (B). $\nabla P$ is a pressure gradient, $\nabla c$ is a concentration gradient, $F_{drive}$ is the driving force, $F_{drag}$ is the viscous drag force, $v_{bub}$ is the bubble's velocity, $v_0$ is the initial component of the velocity of a detached bubble and $\hat{m}$ is the intrinsinc unit vector of the Janus particle which is always $\perp$ to the silica-Pt interface [5].

For a single Janus, it has been seen that higher the concentration of $[H_2O_2]$ is, the higher the velocity achieved. This linear relationship is true until a critical value for $[H_2O_2]$ is reached [6]. Above the critical concentration, the velocity of Janus particles saturates. Therefore, the velocity of Janus particles can be controlled within the system by adjusting the peroxide concentration. In many occasions, this control is critical as the higher $[H_2O_2]$ there is, the higher oxygen bubbles are produced. This oxygen not only will create interfaces that will modify Janus behaviour but also, it will be problematic in

* Electronic address: lpalacru7@ub.edu

many applications. Therefore, an equilibrium between velocity and bubble generation is needed for many of its potential applications.

From an industrial point of view, Janus are the future of better chemical processes but also, a great improvement for health. On the one hand, Janus have been considered to clean waste waters of organic molecules and heavy metal [7]. Because of it self-propulsion, reaction done with this method does not need a stirrer. Also, in the case of organic molecules, there is no need of adding extra chemicals to make the solution acidic as happens now. Moreover, Janus can be reutilizable. On the other hand, Janus may be interesting to drug delivery or cancer treatment [8]. Today, cancer treatment remains primary in surgery and in radio and chemotherapy. These types of treatments have large problems. Invasive surgery can always lead to many difficulties as infections or bleedings that could cause death. Treatments based on radio and chemotherapy have also a negative side. They not only attack malignant cells but also the healthy ones. For example, inmuno cells are very sensible to radiation and thus immune system of patients drops letting to infections problems. Because of these problems, new solutions should be explored. In this case, Janus based on peroxide reaction could be very useful as tumour cells have an overproduction of $H_2O_2$. Therefore, Janus will be mostly active on the surrounding of tumour cells and they will be concentred around tumours. Once attracted to the tumour, multiple options could be considered in order to kill malignant cells. One of these possible modes could be by heating Janus but also, by drug delivery. Drug delivery consists on transporting specifically some quantity of a drug to a specifically destination. This could be possible because of the attraction of a cargo particle to a Janus one. For example, this can be done by applying a magnetic field [9]. Also, this could also be used not only for cancer treatment but in general, for any type of disease reducing therefore, secondary effects associated to medicines. Moreover, more biomedical applications are in mind [8].

From a physical point of view, catalytic Janus particles are very interesting because of their out-of-equilibrium behaviour and because of the collective complex phenomena that could occur in these systems. Due to its shape, Janus movement could lead easily to rotational changes which can characterised their movement causing different trajectory behaviours and different flows in the fluid that surrounds them. Furthermore, clustering is also seen in Janus dilutions. These clusters lead to self-organization [10] and to phase transition as flocking [2]. These phase transitions are seen to be microphase transitions rather than macrophase as there seems to be a limiting size in cluster formation. Therefore, dynamical clustering can be observed where continuous exchange of particles occurs. Studies on phase transitions and self-organization [10] will lead to a better understanding of self-propelled particles, opening the possibility of using them in the previously mentioned applications. Moreover, we cannot forget that the Janus particles will not be in a clean bulk fluid in real applications. Fluids can have lots of compounds and therefore, there will inevitably be different types of interfaces. If a Janus particle reaches one of the interfaces, the related phenomena could change significantly. Therefore, studies of catalytic Janus particles near interfaces are quite interesting. As the Janus particles are diluted in a fluid, one of the compounds of the interface must be a fluid. On the other side, although studies can be done with solid, it is much interesting with another fluid because of the final applications. Because of the above, in this work I will focus on what Janus particles at a liquid-liquid interface. The idea of this work is to start a long study that will characterize this problem not only from an experimental, but also from a theoretical point of view. Nowadays, there exist some models to describe catalytic Janus particles [10] but fundamental parameters present in these models are still unknown to characterize the real Pt-Janus behaviour. Because of this, computer simulations of a Janus model were performed in order to obtain the correct estimates of the needed parameters. Comparisons to reality could not be possible to do it if experiments were not done. As a consequence, preparation of Janus particles and tracking of it was done in order to have physical parameters. Finally, little modifications on the interface were done by the addition of surfactants in the Janus dilution to see the changes in its behaviour as they will decrease surface tension between the two liquids.

Once these questions are answered, we will be able to move onto clusters and phase transitions behaviours in next studies.

## II. EXPERIMENTAL SETUP

### A. FABRICATION OF JANUS PARTICLES

Pt-Janus particles were fabricated in two steps. Firstly, close packed monolayers of 5 μm Ø silica particles were created using a drop-casting method. Right after, 15 nm layer of Pt was deposited over the sample using a spattering (Leica EM ACE600). As samples were only exposed at half of the surface, Pt was deposited only on half of the particles (see Fig. 2). Next, an Ar plasma cleaning was done on the samples as this process is believed to clean the Pt layer. Later, samples were sonicated in vials filled with miliQ water to release the particles from the glass surface and stored at room temperature. Finally, in order to verify that the activity of Janus particles, a small amount of Janus particles (typically 5-10 μl) mixed with $H_2O_2$ was observed under the microscope.

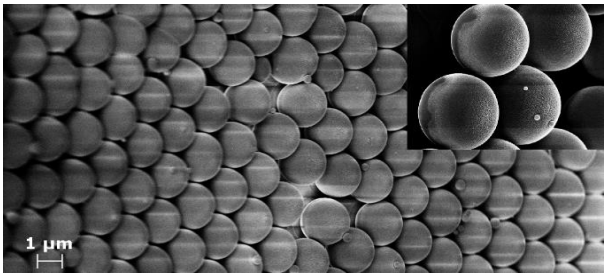


FIG. 2: Pt-silica Janus particles after Pt attack. Insight: Detail of both parts after the attack.

### B. MICROFLUIDIC EXPERIMENTS

Because of its ease of preparation and safety, liquid-liquid interface was created with oil and water. Microfluidics chips were used for interface creation. These chips (ibidi) consist of a 3.8x17x0.4 mm channel with two reservoirs in each of the ends (see Fig. 3). In each channel, 18 μl of Silicon oil 50 cst

(Sigma-Aldrich) was introduced in the middle of the channel. Next, 35 µl of fresh Janus particles dilution with a $H_2O_2$ final concentration of 2.5% (over volume) was introduced in each of the sides. The dilution should be fresh as the Janus particles will degrade $H_2O_2$ over time. Also, in order to avoid self-decomposition of $H_2O_2$, $H_2O_2$ was stored at 4ºC in the fridge. This design of the experiment was carried out in order to avoid bubble accumulation in the middle of the channel. As Janus dilution was near the reservoir, bubbles had more chance to escape and thus allowed for us to avoid movements on the liquid-liquid interface because of bubble enlargement or bubble explosion. Also, by doing this we had two interfaces to perform our observations. Notice that, every time Janus were needed, a 5-minute sonication was performed in order to destroy the particle clusters.

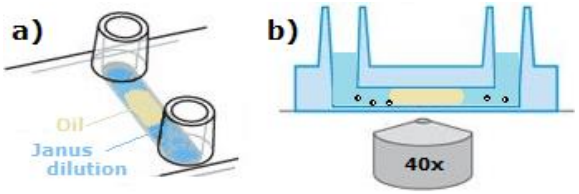


FIG. 3 (Colour online): Microfluidic canal experimental setup. a) Upside view b) Side view

In the case of surfactants dilutions, two types were used but in both cases, final [$H_2O_2$] was of 2.5% (over volume). Firstly, the organic common non-ionic surfactant *Triton-X 100* (Sigma-Aldrich) was used. In this case, final concentration was established to be 0.05% over mass as previous works showed that at this level Janus were moving at maximum velocity [11]. Although it, at the end it was used a concentration of 0.005% over mass because of stabilization problems of the interface. Comments on this problem will be described in section IV. Secondly, common anionic surfactant *Sodium dodecyl sulfate* (SDS) (Sigma-Aldrich) was used. In this case, concentration of SDS on Janus dilution was established to be 0.05% over mass [11].

Finally, experiments were recorded using a contrast microscope (Leica) with a 40x objective. Resulted videos were tracked using tracking software developed by the Smart-Nano-Bio Devices group. Data analysis was performed by a self-custom Matlab software algorithm.

## III. MODEL AND NUMERICAL DETAILS

Although self-propulsion of Pt-Janus particles can be described from different points of view (see Fig. 1), in this work a self-diffusiphoretic model has been chosen not only because of its simplicity to model but also, because of its inherit fundamental physics. In particular, Janus are modelled by means of two major parameters: surface activity (α) and surface mobility (µ) [12].

On the one hand, Pt-Janus need a combustible to move. Here, we suppose that both the combustible and water are in high amount but the product of the reaction is not. As a consequence, if one describes the combustible product as a solute in the fluid it will be able to define a concentration profile *c* which will follow heat equation. Because of Janus production, this profile will change in time continually. Therefore, it is needed to introduce a term that acts as a source in the heat equation. To introduce this, the α term was used. Indeed, this parameter is not introduced in this way but what we called $\mathcal{Q}_C$ as some assumptions must be considered. First, activity is only done in half of the Janus shell. Second, in some occasions as in clustering, Janus can have less activity as they cannot contact at all with the combustible. Consequently, it is needed to introduce a term called $c_*$ that will take this in consideration. By mixing both arguments, it was proposed:

$$\mathcal{Q}_C(\boldsymbol{r},t) = \alpha e^{-\frac{c(\boldsymbol{r},t)}{c_*}} \sum_i^{N_p} \delta\left(\left|r - r^{(i)}(t)\right| - R\right) \cdot \Theta\left(-\hat{m}^{(i)}(t)\left(r \cdot r^{(i)}(t)\right)\right) \quad (1)$$

where $\delta(\cdot)$ is the Dirac's delta, $\Theta(\cdot)$ is the Heviside's theta function and $r^{(i)}$ and $\hat{m}^{(i)}$ are the position and the intrinsic unit vector of the *i*-th colloid at time *t*. In our simulations we will be in a very diluted regime (only one particle) but for generalization, Eq. (1) sums over all $N_p$ particles of radius *R*. On the other hand, if activity is being done during much time, some computational problems could appear because of overflows. In order to solve this point, a sink term ($\mathcal{T}_C$) was also introduced in the heat equation. This term will keep the volume average $\langle c \rangle$ constant in time in order to preserve the conserved dynamics. If the scalar field diffusivity is defined as D, then, our heat equation can be described as:

$$\partial_t c = D\nabla^2 c + \mathcal{Q}_C - \mathcal{T}_C \quad (1)$$

Now, it should be taken the surrounding fluid into account. As the system has the solute and solvent, a strategy to introduce this mixture is needed. One manner to achieve this is by introducing it in a coarsed-grained way by recalling a free energy functional [13] of the form:

$$F = \int dr \left\{-\frac{A}{2}\phi^2 + \frac{B}{4}\phi^4 + \frac{1}{3}\rho\, log\, \rho + \frac{\kappa}{2}|\nabla\phi|^2\right\} \quad (2)$$

where $\phi$ is the order parameter that will describe the mixture, $\rho$ is the total density of the fluid, $\kappa$ is a parameter related to the energy cost of generating a spatial gradient and finally, A and B are parameters that will describe the phase behaviour of the mixture. With this consideration, apart from Eq. (1), Navier-Stokes (NS) equation should be solved:

$$\partial_t \boldsymbol{u} = -\nabla P + \nu\nabla^2\boldsymbol{u} + A\nabla\left(\frac{c^2}{2}\right) \quad (3)$$

where **u** is the velocity field for all the fluid (solvent and solute), *P* is the pressure field and *ν* is the kinematic viscosity. As NS is computationally costly, an efficient algorithm should be chosen. In the late decades, multiples algorithms have appeared to solve NS [14]. As there is the need to introduce the binary mixture through Eq. (2), not every algorithm is capable. One of the late algorithms where this is easy to implement is the known as Lattice Boltzmann (LB) algorithm [14]. LB has the particularity of not solving the problem from a macroscopic point of view but instead, from a microscopic

point of view. Rather than discretising the continuum space from NS, it solves the Boltzmann equation with linear collisions for fictive particles that can move freely:

$$\frac{\partial f}{\partial t} + \boldsymbol{v} \cdot \nabla f + F_{ext} \frac{\partial f}{\partial \boldsymbol{v}} = \Omega \qquad (4)$$

In Eq. (4), f(**r**, $\boldsymbol{v}$, t) is the particle distribution function, $\boldsymbol{v}$ is the particle velocity, $F_{ext}$ is all the external forces applied to the particles and Ω is the collision operator which describes the collision between our fictive particles and which is defined as follows:

$$\Omega = \int dv_1' dv_2' dv_2 \, (f_1' f_2' - f_1 f_2) w_{12 \to 1'2'} \qquad (5)$$

where $f_1'$ and $f_2'$ are the final states of the particles after the collision, $f_1$ and $f_2$ are the initial states, $w_{12\to1'2'}$ is the probability of performing this transition and the integral is done over the velocity space of final states $(v_1', v_2')$ and initial state $(v_2)$. Although the term Ω is quite complex to solve, an approximation can be done. The most known approximation is the BGK, named after its proposal by Bhatnagar, Gross and Krook [15]. They assumed that the effect of molecular collisions is to bring the velocity distribution function closer to the equilibrium distribution. Moreover, they propose that this will happen with a rate proportional to the molecular collision frequency:

$$\Omega = \frac{1}{\tau}(f^{eq} - f) \qquad (6)$$

here, τ is the characteristic time that will pass before two particles collide and $f^{eq}$ is the distribution $f$ at equilibrium. In addition, this algorithm discretize velocity space of the system in a finite number of $v_i$ velocities. As a consequence, space lattice will be also discretized as it will require $x + v_i$ to be again in a lattice position. Therefore, if only integer values of time t are taking then, $f$ must also be discretized. Thus, the change $f(x, v_i, t) \to f_i(x, t)$ and also, $F(v_i) \to F_i$ can be done. By taking $\Delta x = \Delta t = 1$ then, Eq. (4) with the substitution defined by Eq. (6) will transform into:

$$\underbrace{f_i(x + v_i, t + 1) - f_i(x, t)}_{Streaming} = \underbrace{\frac{1}{\tau}\left(f_i^{eq} - f_i\right) - F_i}_{Colisions} \qquad (7)$$

Although this equation seems to be far from NS, in fact, it has all the essence of NS. If relations expressed in Eq. (8) are demanded then, NS is recovered.

$$\sum_i f_i = \rho$$
$$\sum_i f_i v_i = \rho \boldsymbol{u} \qquad (8)$$
$$\sum_i f_i v_{i\alpha} v_{i\beta} = P_{\alpha\beta}$$

Here $\rho$ refers to local fluid density, **u** is the velocity of the fluid and *P* is the stress of the fluid. In order to show this, we can do a Taylor expansion of $f_i^{eq}$ and $f_i$ in terms of the Knudsen number (K) (Eq. 9). K is a dimensionless number defined as the ratio of the molecular mean free path length to the representative physical length scale.

$$f_i = f_i^{eq} + K f_i^{neq}$$
$$f_i^{neq} = f_i^1 + K f_i^2 + O(K^2) \qquad (9)$$
$$\textstyle\sum_i f_i^k = \sum_i f_i^k \boldsymbol{v_i} = 0 \text{ for k=1,2}$$

Now, defining $t_1$ as the convective time-scale and $t_2$ as the diffusive time-scale and by doing a Chapman-Enskog expansion at order two following Eq. (10), one could achieve Eq. (11).

$$\partial_t = K\partial_{t1} + K^2 \partial_{t2}$$
$$\partial_x = K\partial_x \qquad (10)$$

$$\partial_{t_1} \mathrm{f_i^{eq}} + \boldsymbol{v}_i \nabla_1 f_i^{eq} = -\frac{f_i^1}{\tau}$$
$$\partial_{t_2} \mathrm{f_i^{eq}} + \left(1 - \frac{1}{2\tau}\right)\left[\partial_{t_1} f_i^1 + \boldsymbol{v}_i \nabla_1 f_i^{(1)}\right] = -\frac{f_i^2}{\tau} \qquad (11)$$

Next, by making a second order expansion of the equilibrium particle distribution as in Eq. (12), summing Eq. (11) over all particles and applying the conditions in Eq. (8) and Eq. (9), one can recover NS.

$$\mathrm{f_i^{eq}} = \frac{\rho}{(2\pi RT)^{\frac{D}{2}}} e^{-\left(\frac{(v_i - u)^2}{2RT}\right)} = \frac{\rho}{(2\pi RT)^{\frac{D}{2}}} e^{-\frac{(v_i)^2}{2RT}}$$
$$\cdot \left(1 + \frac{\boldsymbol{v}_i \boldsymbol{u}}{RT} + \frac{1}{2}\left(\frac{\boldsymbol{v}_i \boldsymbol{u}}{RT}\right)^2 - \frac{\boldsymbol{u}^2}{2RT}\right) = \qquad (12)$$
$$= \omega_i \rho \left(1 + \frac{\boldsymbol{v}_i \boldsymbol{u}}{c_s^2} + \frac{1}{2}\left(\frac{\boldsymbol{v}_i \boldsymbol{u}}{c_s^2}\right)^2 - \frac{\boldsymbol{u}^2}{2c_s^2}\right)$$

Expansion given in Eq. (12) takes the velocity of the sound ($c_s$) in account. It is important to notice that this expansion is only valid for small velocities and therefore, simulations will be only valid if the fluid and Janus are far away from the speed of the sound of the fluid medium. On the other hand, $\omega_i$ is a weight factor that depends on the velocity vector. In fact, if these equations need to be valid, a small number of different $v_i$ are needed in order to have enough sufficient symmetry to ensure that at the hydrodynamic level the behavior is isotropic and independent of the underlying lattice [16]. Depending on the dimension of the problem, different numbers of $v_i$ and $\omega_i$ are proposed. The most used distributions are shown in Fig. 4. Similar to $f_i$, solute concentration field can be also added to the problem by introducing a new distribution function that we will call $g_i$. In this case, $f_i$ describes the density field $\rho$ and $g_i$ describes the order parameter $\phi$ seen in Eq. (2) [17]. Next, in order to simulate this problem, a two-step procedure over time is perfomed:

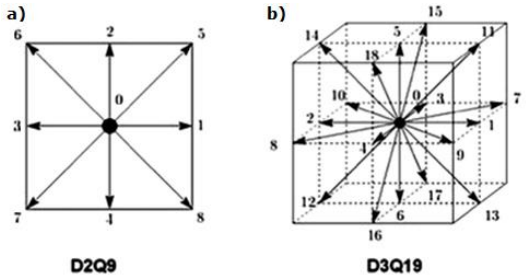


FIG. 4: Discretization of velocity vectors in LB.
a) D2Q9 (2D, 9 $\boldsymbol{v}_i$ components) b) D3Q19 (3D, 19 $\boldsymbol{v}_i$ components)

1. Fictive particles are moved one step following its probability distribution $f_i$ and $g_i$, which will change to $f_i^*$ and $g_i^*$, respectively, in the direction of $v_i$ (Streaming process, see Eq. (7)). Later, using Eq. (8), $\rho$, **u**, $f_i^{eq}$ and $g_i^{eq}$ are recalculated.
2. Collisions are applied into our fictive particles with the new $f_i^*$, $f_i^{eq}$, $g_i^*$ and $g_i^{eq}$ (Collision process, see Eq. (7)).

Until now, Janus have not been introduced in the algorithm. In order to introduce them, it is very important to take boundary conditions of the fluid (BC). Typically, BC consists on the so called bounced-back. If a particle after its stream reaches a forbidden point of the lattice then, the particle is moved again to its previous point. This would happen if a node of the lattice is detected as a solid point, which will be introduced in the case of a having a wall or a Janus particle. Because of collisions against Janus, a force and torque over the particle will be able to be calculated. Both parameters will be used to update Janus position and velocity at each time step. Moreover, it is also needed to impose an extra BC over Janus particles. Theory of colloidal phoresis [18] shows that over a solid particle, there is an effective slip velocity $\mathbf{v}_s$ that can be model from a location $\mathbf{r}_s$ on the particle surface as:

$$\mathbf{v}_s = \mu(\boldsymbol{r}_s)(\mathbf{1} - \hat{r}_s \otimes \hat{r}_s) \cdot \nabla c \qquad (13)$$

Here, $\mu(\boldsymbol{r}_s)$ is constant and therefore, it will be refered as $\mu$. This parameter is the previously introduced as the surface mobility. Values of $\mu > 0$ will denote chemorepellent behaviour and values of $\mu < 0$, chemoattractive. As Janus have two different sides, Janus will be modelled by using two pairs of the above parameters: $\alpha_1$, $\mu_1$ for the passive part and $\alpha_2$, $\mu_2$ for the active part.

By this way, mesoscopic equations can be simulated but with the advantages of the microscopic point of view. Because of its mode of work, binary mixtures are easy to simulate and therefore, complex phenomena are. Moreover, the two-step implementation leads to run this algorithm in a parallel way, which is needed for supercomputer utilization. As there is much complexity in setting up all the algorithm, in this case "Ludwig" software [17] has been adopted (Statistical group of physics, Faculty of physics, UB). Minor changes of the software called "Ludwig" were performed. Over all, computer simulations were done with a $46^3$ lattice using 4 processors at time. Only one Janus was simulated at time as the diluted regime was studied.

## IV. EXPERIMENTAL RESULTS

First experiments with Janus particles showed that they sediment to the bottom of the channel. Once there, Janus particles did not vary in the z-plane. Most of the particles had their intrinsic unit vector $\hat{m}$ (see Fig. 1) parallel to the z-plane, although some were perpendicular. In the first case, 2D motion was observed, including angular reorientation within the x-y plane. In the second case, neither propulsion nor rotation was seen. It has to be noted that bubbles formation can be a significant challenge in studying the motion of Janus particles. It was expected to solely observe auto-propelled movement but at the end, one should differentiate this movement from the one created as a consequence of flows generated by bubbles. In some occasions, the Janus particle movement was in a different direction from its m^. In that cases, data was discarded as there must necessarily be some flow in order to let the Janus move in that direction. In other cases, Janus movement was accepted as self-propelled but the presence of some kind of flow that moves the particles in the same $\hat{m}$ direction cannot be discarded. After tracking analysis, its behavior was studied by fitting MSD with the following equation:

$$MSD = 4D\Delta t + v^2\Delta t^2 \qquad (14)$$

where $D$ is the diffusion coefficient of the Janus and $v$ is its velocity. This approximation can be done as we are taking in account $\Delta t \ll \tau_R$, where $\tau_R$ is a characteristic time defined by the inverse of rotational diffusion coefficient [7], which in this case is about 100 s. In Fig. 5 all fits are presented and in Table I and II, velocities and $D$ are shown.

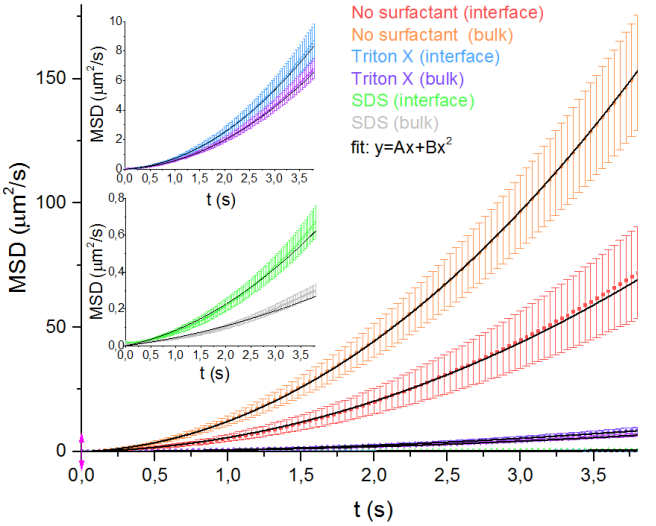


FIG. 5: (Colour online): MSD of Pt-silica Janus particles at the oil-water interface and in the bulk. Red: Without surfactant, interface. Orange: Without surfactant, bulk. Blue: Triton X, interface. Violet: Triton X, bulk. Green: SDS, bulk. Grey: SDS, interface. Inset: Zoom-in of the MSD plots for surfactants conditions.

| | Bulk | Interface |
|---|---|---|
| Without surfactant | 3.17±0.03 | 2.12±0.02 |
| Non-ionic surfactant (Triton X) | 0.643±0.008 | 0.73±0.01 |
| Anionic surfactant (SDS) | 0.097±0.006 | 0.169±0.005 |

TABLE I. (In colour) Janus velocity for the different studied systems. Units are in μm/s. Red: Values not acceptable.

| | Bulk | Interface |
|---|---|---|
| Without surfactant | 0.55 ± 0.04 | 0.30 ± 0.02 |
| Non-ionic surfactant (Triton X) | 0.040 ± 0.003 | 0.050 ± 0.004 |
| Anionic surfactant (SDS) | 0.0090 ± 0.0005 | 0.0140 ± 0.0008 |

TABLE II. (In colour) Janus diffusion coefficient for the different studied systems. Units are in $\mu m^2/s$. Red: Values not acceptable.

In the case of the bulk, the Janus particles had a velocity of 3.17 ± 0.03 µm/s. As the particles are 5 µm in diameter, it can be seen that these artificial micromotors can move approximately 0.6 its body length/s. If one compares this data to natural micromotors, one could see that this is not very comparable. For example, one of the fastest and studied bacteria, V. alginolyctus, can move at speeds of 60 µm/s. Moreover, there are even faster bacteria as P. haloplanktis which can move at speeds up to 100 µm/s [19]. Neither of them are bigger than 10 µm and therefore, natural microswimmers can lead to movements of 10 its body length/s. Nevertheless, Janus are much simpler and could be more useful than bacterium in many practical cases. For example, in medicine Janus will not be detected by inmuno system as bacterium would be.

After the study of Janus particles in the bulk, the interface study was performed. As Janus particles sediment, a pure oil-water interface was not possible to be created perfectly and a triple interface had to be created: oil-water-hydrophilic polymer (from the bottom of the chip). In order to avoid this extra interface, two ideas were tested. On the one hand, a water/oil horizontal interface was considered. Although the particles sediment, it was thought that they will not go through oil in a long time scale allowing for enough time to track their motion over the interface due to interfacial force as it will be stronger than the gravitational force applied on the particle. Therefore, water should be above the oil as they will sediment in water part. Unfortunately, no commercial oil was found to be denser than water. Other liquids denser than water but not mixable with water were considered. Unluckily, all other liquids found were very toxic. One of the less, but still, toxic liquids, was chloroform. It was considered to be used but at the end, it was discarded because $H_2O_2$ is a very oxidizing compound and in contact with chloroform, an explosion would have happened. Although not a liquid, it was also considered to perform an air-water interface as both are fluids. This last strategy could not be done because no objective for the microscope with enough high focal distance was available in the lab.

On the other hand, it was also proposed to attach the oil at the bottom by capillarity forces (see Fig. 6). This was tried by fabricating cylindrical PDMS chambers. Next, the PDMS structure was attached to crystal coverslips by performing an oxygen plasma activation for 30 seconds. After, a transmitted electron microscope (TEM) membrane was placed at the bottom of the hole. Next, oil was introduced into the membrane and a drop of Janus dilution was put over the oil. No successful result was obtained as the water-oil interface dismantled very quickly. However, this system can be refined in the future to obtain more stable oil-water interfaces as a variation of this setup, it was also proposed to attach PDMS holes into flat and thin PDMS layers. In that case, plasma cleaner was performed for 5 minutes as PDMS is very hydrophobic. Attachment of both parts was difficult but possible. Nevertheless, the water-oil interface dismantled again.

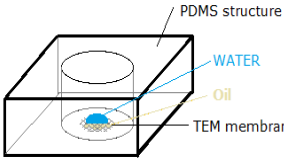


FIG. 6 (Colour online): Montage of experiment to attach oil to the bottom.

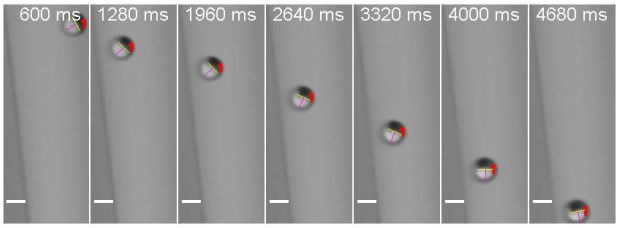


FIG. 7: Approaching of Pt-Janus to the oil-water interface. Scale bar is 5 µm

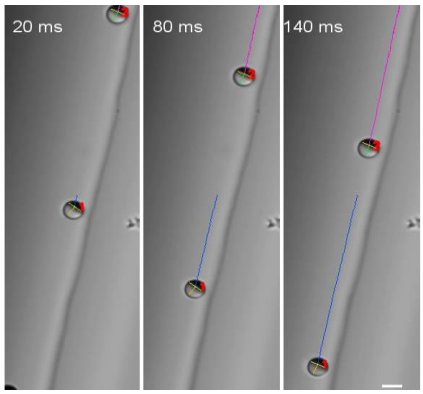


FIG. 8: Movement of Pt-Janus at the oil-water interface. Scale bar is 5 µm

Although we had the triple interface in our set up with the microfluidic chip, we decided following with the experiments and tracking of Janus at the oil-water- hydrophilic polymer interface. When the Janus particles approach the oil surface, a reorientation of the particle was seen (see Fig. 7). After the reorientation, the particles did not leave the interface if the path was free (see Fig. 8). Angular fluctuations also decreased significantly at the interface as compared to the bulk (see Fig. 9). As it can be seen in both the previous figures, the particle does not seem to be touching the interface but it is close to it. In fact, it was measured a distance of 2.3 ± 0.2µm or, what is the same, 0.94 ± 0.06 R. This result leads us to think if the particle would stabilize at a distance of its own radius. As a consequence, more analysis should be done with different sizes of Janus particles. In any case, this separation could be because of some hydrodynamic interaction or even because the Janus is touching the oil surface. This last option cannot be

discarded as it was seen that oil has higher angle contact than water. Therefore, as oil-water interface is not flat but curved, this could lead to a contact at the top of the particle that could attract it. Side view experiments should be performed in order to discard, or verify, this last hypothesis. However, it could not be done during the current project. Rarely, detachment was seen as a consequence of trash or other Janus particles present in the path of the observed particle. Those cases were not tracked as they do not represent the fundamental behavior. In the rest of cases, velocity and angle of Janus were seen to be constant when recording. When velocity was calculated (see Table I), a reduction of 33% was calculated with respect to the bulk conditions. On the other hand, D (see Table II) was also around 45% less than in respect with bulk. As a consequence, experiments at the liquid-liquid interface must take into account, these decays.

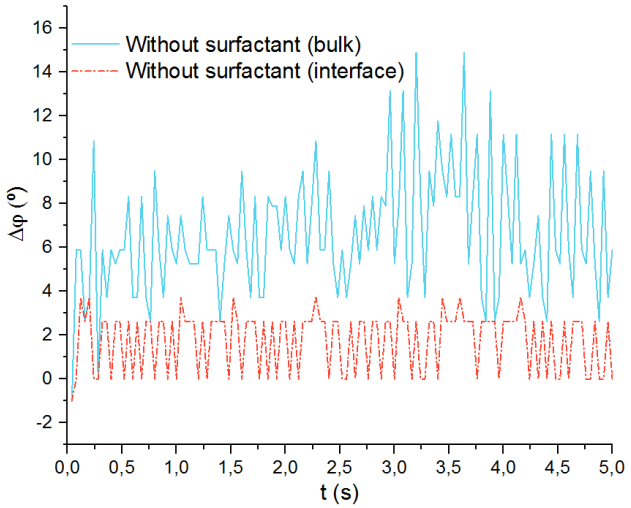


FIG. 9: Example of fluctuations of Janus particles at the bulk (continuous line) and in the interface (dashed line). Particles chosen are representative of Janus behaviour in both conditions.

After performing these experiments, some variations were introduced on the interface with the use of surfactants. First, a non-ionic surfactant (Triton X) was added. At initial concentration (0.05% over mass) of study, interface was very difficult to be observed. In fact, oil 'seemed' to be much less viscous as it could move incredible fast inside the channel. A hypothesis to explain this fact could be that oil is not less viscous but is not in contact with walls of the channel, allowing it to float inside water. This could explain why sometimes one could see Janus in the oil part, especially in the borders. Moreover, by adjusting finely the contrast of the image, sometimes one could see that these particles moving in the oil region were not at all in the oil as some solid fringe of oil appeared beyond the particle position. As a consequence, dilution was reduced 1/10 as still, it should be seen an effect of surfactant [11]. With the new concentration, Janus were tracked again. In this case, it was seen that particles still can be attached to the interface but bigger dispersion related to the distance of the Janus to the liquid interface was found. It was estimated that Janus were at a 3.7 ± 0.4 μm, which turns into 1.5 ± 0.2 R. In any case, this value is significant higher than 1 R of distance, which was the result that we obtained for the non-surfactant case. When velocity for bulk was measured, a decay of 77% was observed. This is not surprising as the surfactant interferes in the catalysis of the $H_2O_2$ [11]. On the other hand, what was surprising to find was an increase of 12% of the velocity and 20% of D at the interface in comparison with the bulk. Surfactants should reduce interfacial energy [20] and thus, particles should be more free as we found with the increase of width between them and the wall. Moreover, if they are freer, they should move faster comparing with the non-surfactant condition but nothing more was expected. With these results, two hypotheses can be done. The first one is that, although it is not appreciable, there is always a flow produced in the interface, which push particles and therefore, they are faster. Even in the case of having flows, this hypothesis should not be correct because on average, there should not be any difference. A second hypothesis could be that as surfactant is changing interface conditions, it could cause that hydrodynamics produced near the interface are now positive for particle velocity contrary to what it was shown in non-surfactant condition. Additional studies should be done in order to verify them.

Next, in order to see if ions could develop an important role on Janus movement at the interface, SDS surfactant was tried. Janus speed at bulk was significantly lower as it was expected [11]. When oil was introduced, the formation of liquid-liquid interface was still possible although it appeared a small sinusoidal fluctuation on the interface. Although its addition, Janus were still moving along the interface without escaping. When distance was measured, it was found that it was bigger than without any surfactant as it was obtained a value of 4.0 ± 0.2μm or, 1.60 ± 0.08 R. As a consequence of anionic surfactant, particles are less attached to the interface but not more than with a non-ionic surfactant. Surprising, we found again that particles were moving faster at the interface rather the bulk. Nevertheless, the parameters found for velocity using Eq. (14) are too small to consider them true. We cannot forget that we are recording videos with an optical microscope without fluorescence. As these types of microscope have a resolution of the wavelength of light/2, this would let us a down limit of ~150 nm for UV, illumination which we did not use. As D is also taken in account from the same previous fit, we are skeptical of accepting this value as well.

## V. COMPUTATIONAL RESULTS

Janus particles need two pairs of values (α, μ). Here, passive part was chosen to be the first pair leading the second pair to be the active part. As Pt-Janus only do reaction on one side of the particle, it was set to zero the value of $\alpha_1$. Moreover, an initial hypothesis was done by considering that mobilities on both sides should be similar and therefore, $\mu_1 = \mu_2$. With these considerations, firsts attempts to understand control parameters started with the understanding of $(\alpha_2, \mu_2)$ limit values. In order to verify appropriate limits for simulations, velocity of the Janus was chosen as a test as auto-propelled particles should have low Péclet number (Pe). Pe is described as a relation between the characteristic diffusive time of the chemical field and the one from the displacement of the particle. Therefore, this number is described following:

$$\mathrm{Pe} = \frac{\mathrm{vR}}{\mathrm{D}} \qquad (14)$$

where v is the velocity of the Janus, R is the radius of the Janus and D is the diffusivity of the chemical field. In order to do our simulations, a Pe<1 was considered. As a consequence, values for R and D should be considered. The former has much discussion because it is critical for Janus simulations. Low values of R are not desirable because the smaller is R, the less nodes of fluid contact with the Janus. If low number of nodes are in contact, the particle will not interact correctly with the fluid causing a bad interpretation of the Janus behavior. On the contrary, if R is chosen high, higher lattice dimensions should be chosen, which in turn will slow more computer simulations. Moreover, if R is increased, v will slow as major friction will be applied and therefore, computer simulations will also be slower because it will take longer to stabilize the system. The latter is also important for modulating Pe. D can be obtained by recalling Cahn-Hilliard equation:

$$j = \mathrm{M}\nabla\mu = \mathrm{M}\frac{\partial\tilde{\mu}}{\partial\phi}\nabla\phi = \mathrm{MA}\nabla\phi = D\nabla\phi \qquad (15)$$

where $j$ is the flux caused by the order parameter $\phi$, M is the mobility of the fluid, $\tilde{\mu}$ is the chemical potential and A is the factor proportional with $\phi^2$ in the functional that defines the free energy of this model. At the end, in order to fulfill Pe<1, it was chosen D = 0.125 and R=4.5, both in natural units of LB. With these considerations, it was also guaranteed that neither the velocity of the fictive particles of the fluid will exceed low Mach number as required by LB algorithm. Next, simulations over broad range of $(\alpha_2, \mu)$ were considered. Regarding the results, it was concluded that following simulations should be done with $\mu_{1,2} \in [-0.05, 0.05]$ and $\alpha_2 = 0.005$.

Once primary parameters were determined, interface studies were introduced. As it was impossible to determine experimentally a liquid-liquid interface, first, it was proposed to study a solid-liquid interface as this was able to be obtained in the case of Janus in the bulk, where they were in the interface between the polymer and the water solution with hydrogen peroxide. As a result, a solid wall was introduced in each of the extremal z planes. Then, Janus were located at 1.8 R far from the wall and oriented with $\hat{m} = \hat{x}$. With walls, the condition of $\mu_1 = \mu_2$ was relaxed and it was looked for differences of behavior depending on the values of both $\mu_{1,2}$. As a result, $\mu_1$ was fixed and $\mu_2$ was varied. This condition was repeated later for different cases of $\mu_1$. From the above simulations, there were seen several interesting behaviors. First, it was shown that in general, Janus can stabilize its distance from the wall if it is enough near to it, without the necessity of feeling the gravity (see Fig. 10 and 11). In fact, in many of the simulations there was not found any difference between both cases. When distance was studied, several cases were seen. In general, the stabilization occurs with a very close distance from the wall, within less than 0.3R of separation between the wall and the border of the Janus. This limit is important to see as experimental data has showed that particles are at 0.2R from the wall (data not published yet). Although it is true that simulations can have associated an indetermination due to the geometry considered, this value is of the order of $R/L$, where L is the dimension of the box simulated. Therefore, numerical error can lead only to describe a distance of 0.02R, which is much smaller than the distance that it was found. As a consequence, it can be concluded that there is a real separation from the wall due to hydrodynamic interactions. In some occasions, this stabilization occurs for smaller values than 0.02R, which lead to think that there is not a real separation from the wall. This was seen for big positive values of $\mu_2$ when $\mu_1$ was positive. In other cases, bigger values than 0.3R were found. This was the case for small positive values of $\mu_2$. In this case, if $\mu_1 < 0$ it can be seen that stabilization can occur at any value but will not occur in our simulations because of the small dimension of the box simulated. This could be deduced by taking polar angle study in account (see Fig. 12). When $\mu_1 < 0$ and $\mu_2 > 0$ was chosen, angle was stabilized at $\theta = 180º$, even if no equilibrium was seen. Because of it, we deduced the previous hypothesis as when trajectory was seen, particles rotate first to this angle and then, they find its equilibrium from the wall stopping at all. In fact, after deducing this, some simulations with a bigger lattice were done and as a consequence, some new equilibrium points were found. Interesting, this behavior seems to differentiate between introducing gravity and not and also, it breaks at $\mu_1 = 0$, which could induce the ide idea that there is a phase transition at this point. This was also in line with angle analysis as from $\mu_1 = 0$, angle start to reduce. Nevertheless, $\mu_1 < 0$ seems to be not important at all as movement seen was not observed in reality. Only the 180º stabilization case could be used to explain why sometimes Janus appeared experimentally all black, showing all its Pt part from above without any movement. On the contrary, if $\mu_1 > 0$, it does not seem to be this behavior although particles are further than 0.3R from the wall. Surprising, in this case particles with gravity equilibrates at higher distance than without. Despite of being completely different from the previous case, from angular studies (see Fig. 13) it was found that this region was much interesting as Janus started to rotate until, for some values of $\mu_2$, there was found an angle bigger than 90º but smaller than 120º. In this region, particles could move naturally along the wall and against the active part. This was in line with other studies in which chemorepellent behavior of mobilities was needed to understand nature [21]. It is true that this angle could also be seen for some values of $\mu_1 < 0$ but in those cases, particles were moving into the active part side, which has no sense. Unluckily, these correct cases stabilize at higher distances than expected from experimental analysis. In order to solve this problem a lower value of $\mu_1$ could be tried as it was seen that the bigger is $|\mu_1|$, the bigger equilibrium distance is found in general. Nevertheless, it is also true that the bigger is $\mu_1$, the smaller is this region. Because of it, maybe some attraction force should be considered to introduce in the model.

Although stabilization was seen for many values, for some parameters this was not possible to be seen. In particular, there was found a region for small negative $\mu_2$ in the case of $\mu_1 < 0$ and also for small $|\mu_2|$ in the case of $\mu_1 > 0$. In those cases, it can be seen that polar angle stabilization is found between 120º and 180º or between 15º and 90º. Interesting, the bigger $|\mu_1|$ is tried, the bigger range of values is found.

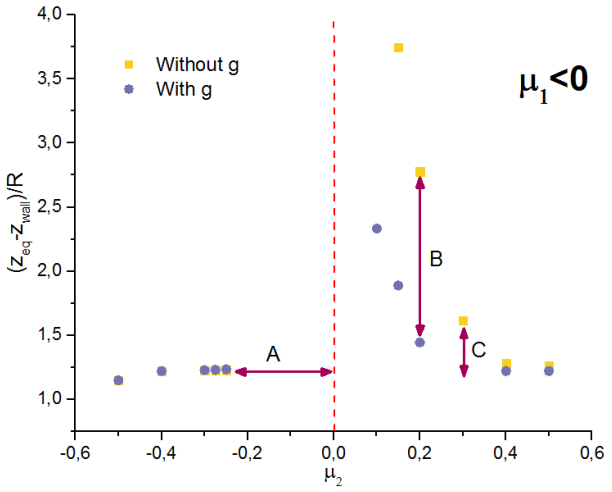


FIG. 10: Janus equilibrium position from a wall in the z-plane. Simulations are done with gravity (blue dots) and without (yellow squares) for $\mu_1 < 0$. No difference between them were found for $\mu_2 < 0$. A: Region with no equilibrium found. The bigger is $|\mu_1|$, the major it is. B: Difference due gravity. C: Height depend on $|\mu_1|$. The higher it is; the higher point is found.

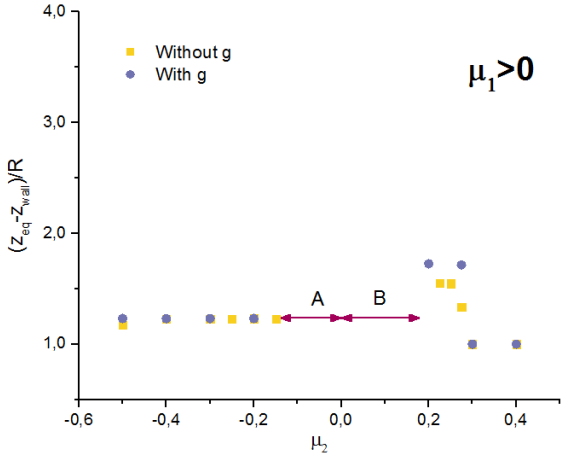


FIG. 11: Janus equilibrium position from a wall in the z-plane. Simulations are done with gravity (blue dots) and without (yellow squares) for $\mu_1 > 0$. A and B: Region with no equilibrium found. A and B grow as $|\mu_1|$ grows but A does in a much slower way.

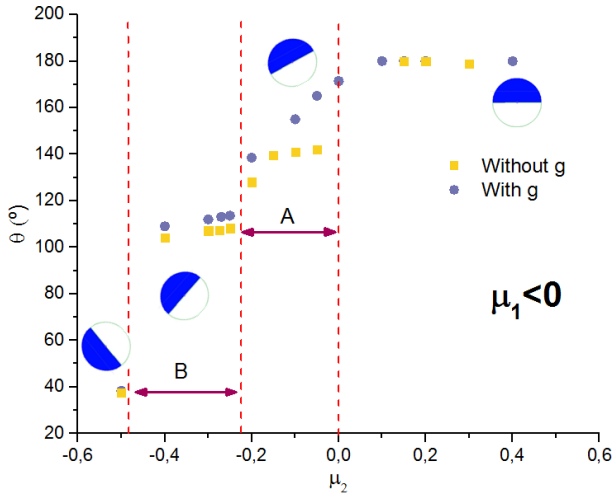


FIG. 12: Janus angle equilibrium reached near from a wall in the z-plane. Simulations are done with gravity (blue dots) and without (yellow squares) for $\mu_1 < 0$. A: Region corresponding with no z equilibrium. The bigger is $|\mu_1|$, the major it is. B: Region with Janus moving along the wall. The bigger is $|\mu_1|$, the major it is. Beyond B, it seems that Janus also move along the wall but with a different configuration.

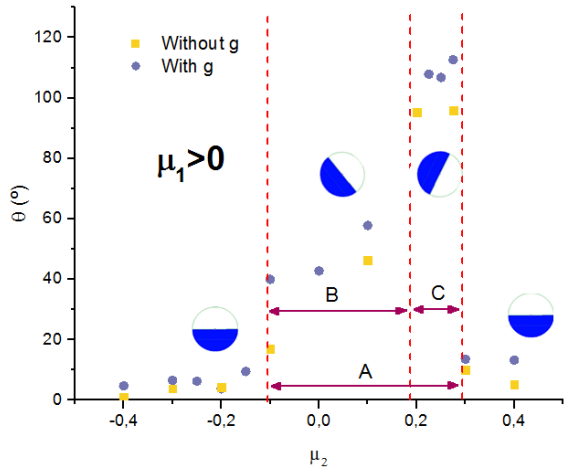


FIG. 13: Janus angle equilibrium reached near from a wall in the z-plane. Simulations are done with gravity (blue dots) and without (yellow squares) for $\mu_1 > 0$. A: Region with different angle stabilization from 0º. The bigger is $|\mu_1|$, the major it is. In this region, if angle is less than 90º (B), stabilization on z is not reached. If angle is between 90º and 120º (C) stabilization is reached and Janus moves according to experimental data.

## VI. CONCLUSIONS & OUTLOOK

In this project we have started a long study on Janus particles from a physical point of view to understand its fundamental behaviour. At the moment, diluted regime near liquid-liquid interfaces has been considered but further work will address in complex phenomena. On the one hand, experimental approximation has showed how Janus particles feel attraction to liquid-liquid interfaces as once they reach one, it is difficult for them to detach by its own action. Differences in its behavior have been demonstrated with velocity and diffusion coefficient where high decreasing rates has been observed. Moreover, it has been showed how Janus stabilizes its angle while they are attached to the interface. Surfactant modifications have shown how, although interfacial energies are modified causing Janus particles to be furthest from walls, Janus particles still feel the needed attraction to do not free from walls. Surprising, we found higher velocities at the interface rather than at the bulk, which still is not very clear the cause behind it. On the other hand, computational simulations have shown how diffusiphoretic models can predict Janus particle behaviour at the solid-liquid interface. In this case, by selecting both mobilities as chemorepellent, we have been able to see the correct movement although not as near from the wall as we would like to see them. Furthermore, depending on their strength, we have been able to change polar angle of Janus particles. In order to achieve this correct movement, polar angle should be between 90º and 120º. Other regions for mobilities have also been studied although not much coincidence with nature has been observed. Only for the case in which Janus oriented with a $\theta = 180º$, some particles can be observed. Although we have not got enough time to

perform liquid-liquid interface studies, we are optimist in with respect this matter as bulk conditions have been demonstrated.

**Acknowledgments**

I would like to thank Dr. Pagonabarraga and Dr. Sánchez for all their advice during this project and because of the opportunity that they give me to do my final year project in their respective teams. Also, I would like to thank Dr. A. Scagliarini and Dr. Alarcon for all their support with computational simulations. Finally, I would like to thank Jaideep Katuri for all his advices in experimental research.

---

[1] Caltech. "There's plenty of room at the bottom" Caltech, [On line]. Available: http://www.its.caltech.edu/~feynman/plenty.html

[2] Sriram Ramaswamy. "The Mechanics and Statistics of Active Matter". Annu. Rev. Condens. Matter Phys. **1**: 323–345 (2010).

[3] C. Casagrande, P. Fabre, E. Raphaël and M. Veyssié, "'Janus Beads': Realization and Behaviour at Water/Oil Interfaces". EPL, **9**: 251-256 (1989).

[4] Aidan T. Brown et al.. "Bulk ionic dissociation is crucial for undestanding chemically-propelled swimmers". arXiv:1512.01778 (2016).

[5] Samuel Sánchez, Lluís Soler, and Jaideep Katuri. "Chemically Powered Micro- and Nanomotors", Angewandte Chemie International Edition **54**: 1414-1444

[6] Jonathan R. Howse, Richard A.L. Jones, Anthony J. Ryan, Tim Gough, Reza Vafabakhsh and Ramin Golestanian. "Self-motile colloidal particles: from directed propulsion to random walk", Phys. Rev. Lett. **99**: 048102 (2007).

[7] Gao W et al. "Seawater-driven magnesium based Janus micromotors for environmental remediation", Nanoscale. **5**: 4696-4700 (2013).

[8] Bradley J. Nelson, Ioannis K. Kaliakatsos and Jake J. Abbott. "Microrobots for minimally invasive medicine", Annu. Rev. Biomed. Eng. **12**: 55–85 (2010).

[9] Larysa Baraban et Al. "Catalytic Janus Motors on Microfluidic Chip: Deterministic Motion for Targeted Cargo Delivery", ACS Nano, **6**: 3383–3389 (2012).

[10] Rodrigo Soto et Al. "Self -assembly of catalytically active colloidal molecules: Tailoring activity through surface chemistry", Phys. Rev. **112**: 068301 (2014).

[11] Juliane Simmchen et Al. "Effect of surfactants on the performance of tubular and spherical micromotors – a comparative study", RSC Adv. **4**: 20334–20340 (2014).

[12] A. Scagliarini, I. Pagonabarraga. "Non-equlibrium phase transitions in suspensions of self-propelled colloidal particles: role of phoretic mobility and hydrodynamics", arXiv:1605.03773 (2016).

[13] Ignacio Pagonabarraga, Alexander J. Wagner, and M. E. Cates. "Binary Fluid Demixing: The Crossover Region", Journal of Statistical Physics, **107**: 39-52, (2002)

[14] Burkhard Dünweg and Anthony J.C. Ladd. "Lattice Boltzmann Simulations of Soft Matter Systems", Advances in Polymer Science: 1-78 (2008)

[15] Bhatnagar, P.L., Gross, E.P and Krook, M., A model for collisional processes in gases I: small amplitude processes in charged and in nutral one-component systems, Phys. Rev. **94**: 511-525 (1954).

[16] Y. H. Qian, D. d'Humières, and P. Lallemand. "Lattice bgk models for navier-stokes equation," EPL (Europhysics Letters), **17**: 479, 1992.

[17] Jran-Christophe Desplat, Ignacio Pagonabarraga and Peter Bladon. "LUDWIG: A parallel Lattice-Boltzmann code for complex fluids", Computer Physics Communications **134**: 273-290 (2001).

[18] John L. Anderson. "Colloid transport by interfacial forces", Ann. Rev. Fluid Mech. **21**: 61-99 (1989)

[19] K.M. Taute, S. Gude, S.J. Tans & T.S. Shimizu. "High-throughput 3D tracking of bacteria on a standard phase contrast microscope", Nature Communications **6**: 8776 (2015).

[20] P. Posocco, A. Perazzo, V. Preziosi, E. Laurini, S. Pricla and S. Guidoc. "Interfacial tension of oil/water emulsions with mixed non-ionic surfactants: comparison between experiments and molecular simulations", RSC Adv., **6**: 4723-4729 (2016)

[21] Juliane Simmchen, Jaideep Katuri, William E. Uspal, Mihail N. Popescu, Mykola Tasinkevych & Samuel Sánchez. "Topographical pathways guide chemical microswimmers", Nat. Commun. **9**; 10598 (2016)